

Analyst

Accepted Manuscript



This is an *Accepted Manuscript*, which has been through the Royal Society of Chemistry peer review process and has been accepted for publication.

Accepted Manuscripts are published online shortly after acceptance, before technical editing, formatting and proof reading. Using this free service, authors can make their results available to the community, in citable form, before we publish the edited article. We will replace this *Accepted Manuscript* with the edited and formatted *Advance Article* as soon as it is available.

You can find more information about *Accepted Manuscripts* in the [Information for Authors](#).

Please note that technical editing may introduce minor changes to the text and/or graphics, which may alter content. The journal's standard [Terms & Conditions](#) and the [Ethical guidelines](#) still apply. In no event shall the Royal Society of Chemistry be held responsible for any errors or omissions in this *Accepted Manuscript* or any consequences arising from the use of any information it contains.

Cite this: DOI: 10.1039/c0xx00000x

www.rsc.org/xxxxxx

ARTICLE TYPE

Binary DNA hairpin-based colorimetric biochip for simultaneous detection of Pb²⁺ and Hg²⁺ in real-world samples

Xiaoli Shi,^a Xiaoyi Gao,^a Lingling Zhang,^a Yunchao Li,^{a,*} Louzhen Fan^a and Hua-Zhong Yu^{b,*}

Received 20th January 2015, Accepted Xth XXXXXXXXXX 20XX

DOI: 10.1039/b000000x

A microarray-format colorimetric biochip was constructed on plastic using two specially-designed DNA hairpin strands as binary probes and a binding-induced conformational switching strategy as the signal generation protocol. Coupled with single- or dual-color staining, we were able to simultaneously detect and quantitate trace amounts of Pb²⁺ and Hg²⁺ in various real-world samples.

Introduction

With the ever increasing pollution from today's industrial production, such as smelting, energy generation and consumption, heavy metal contaminants have spread widely through air, water and soil, posing severe adverse effects on human health and ecosystems due to their high and persistent toxicities.¹ Therefore, it is of importance to develop on-site detection methods that can rapidly analyze heavy metal ions (especially mercury and lead, the two widespread heavy metal contaminants that cause serious human health problems even at low concentrations^{1b}) in complex environmental, biomedical, and food media. The established detection methods for Pb²⁺ and Hg²⁺ include atomic absorption spectrometry (AAS),² inductively coupled plasma mass spectrometry (ICP-MS),³ anodic stripping voltammetry (ASV),⁴ organic ligand-based fluorescent sensors,⁵ DNA-based fluorescent⁶ or electrochemical sensors⁷, and gold nanoparticle (GNP) or enzyme-based colorimetric sensors.^{6a, 8} However, regardless these traditional AAS, ICP-MS and ASV methods or the recently-developed fluorescence and electrochemical methods, they all require specialized instrumentation and trained personnel, and can only be performed in well-equipped laboratory settings. In contrast, colorimetric sensors allow spectrometer-free detection of Pb²⁺ and Hg²⁺, which are particularly suitable for on-site applications. However, it should be pointed out that their sensitivity and selectivity are generally not high.

Another challenge is the identification and quantitation of different ions in multiplexed samples. In fact, the simultaneous detection and discrimination of Pb²⁺ and Hg²⁺ have been actively

explored in the past decade.^{5a, 6b, 6f, 7d, 7e, 8b, 9a, 9b} Chung et al. fabricated two aptamer-functionalized GNP probes with different dye modifications for their fluorescent detection at different excitation wavelengths;^{6f} Zhang et al. constructed a paper-based electrochemiluminescence (ECL) device for their simultaneous detection by a potential-control technique.^{7e} With the help of masking /activating reagents, Chang et al. created a thrombin-binding aptamer-based fluorescence sensor for the detection of the two metals;^{6b} Lin et al. designed an impedimetric DNA sensor for the simultaneous detection of Pb²⁺, Hg²⁺ and Ag⁺.^{7d} Despite the significant progress, we note that either specialized equipment or additional masking/activating reagent is required to achieve simultaneous detection of both ions.

In this paper, we describe a novel binary DNA hairpin-based plastic biochip for the simple, rapid, sensitive and parallel detection of Pb²⁺ and Hg²⁺ based on specific colorimetric reactions. In order to construct such a biochip, two specially designed DNA hairpin probes containing guanine (G)-rich or thymine(T)-rich fragments and with amino and biotin modifications at the two termini, were immobilized on a disposable, plastic chip for recognizing Pb²⁺ and Hg²⁺, respectively. The immobilized DNA probes are initially in their folded forms; upon binding with Pb²⁺ and Hg²⁺, their hairpin secondary structures are "forced" to open, allowing nanogold-streptavidin conjugate (or streptavidin-horseradish peroxidase conjugate) to attach to the biotin groups and produce visual signals thereon upon staining (Scheme1). Because the two probes can be immobilized at specific locations, the biochip has the capability to simultaneously identify and quantify Pb²⁺ and Hg²⁺ in their binary mixtures. To the best of our knowledge, this is the first example of utilizing a microarray-format DNA hairpin-based colorimetric biochip for the parallel detection of multiple heavy metal ions, thus opening a new pathway toward simple, rapid and sensitive on-site analysis of multiplexed samples.

Experimental Section

Fabrication of DNA hairpin biochips: Before probe immobilization, PC substrates were irradiated in a UV/ozone cleaner for 15 min to generate high-density carboxylic acid groups, followed by immersion in a 0.1 M phosphate buffer at pH 6.0 containing 5.0 mM EDC and 0.3 mM NHS for 3 h. After the activation steps, the G-rich DNA probes and T-rich DNA probes (Table S1, ESI[†]) were diluted to 10 μ M with 10 mM Tris coupling buffer (containing 50 mM MgCl₂, pH=7.4) and 20 mM phosphate coupling buffer (containing 150 mM NaCl, 50 mM MgCl₂, pH = 7.4), respectively, and delivered onto the activated PC surface using a polydimethylsiloxane (PDMS) plate with embedded microchannels. The PC chip was then kept in a humidity box for 4 h to form the probe line arrays. The PC chip was rinsed thoroughly with 10 mM Tris buffer and immersed in a blocking buffer (containing 10 mM Tris, 150 mM NaCl, 3% BSA, pH = 7.4) for 2.5 h to passivate the surface. After washing, the samples containing different concentrations of Pb²⁺ and Hg²⁺ were introduced into the channels and kept for 30–45 min. Afterwards, the PDMS plate was peeled off and the plastic chip was washed with Tris buffer again. Finally, the biochip was immersed in a solution containing streptavidin-GNP (or streptavidin-HRP) conjugates for 30–45 min and subjected to silver (or TMB) enhancement. **Color staining:** After incubation with the sample and signal triggering unit, the biochips are ready to stain in order to obtain the visual signals. Before staining, the biochips need to be washed thoroughly with deionized water to remove all interfering anions. They were then immersed in a freshly made silver enhancement solution consisting of silver salt and reducing agent for 10–25 min or 1-component TMB membrane substrate solution for 3–10 min. It is noteworthy that both the silver enhancement solution (after mixing) and the 1-component TMB substrate solution must be replaced with a fresh solution every 10 min in order to obtain satisfactory results.

Parallel detection of Pb²⁺ and Hg²⁺: For the parallel detection of Pb²⁺ and Hg²⁺, the GG-6b and TT-7b probes were immobilized at different locations of an activated PC substrate using a PDMS stamp to form the Pb²⁺ and Hg²⁺ testing zones (in line array format). Afterwards, the samples containing different concentrations of Pb²⁺ and Hg²⁺ were delivered across these testing zones in the direction perpendicular to the probe arrays using another PDMS stamp. The recognition reactions between the two probes and the two target ions occurred at the intersections of the microchannels on the second PDMS plate and the preformed probe line arrays, resulting in the formation of two-dimensional binding arrays thereon. **Signal readout and data analysis:** After staining, the biochips were scanned with a flatbed scanner in reflection mode. The images can be obtained in

either grayscale or color mode, which are subsequently analyzed with an image-processing software program (e.g., Adobe Photoshop). In particular, the average luminosity (I_s) of each binding strip/spot was measured using the histogram tool in Adobe Photoshop and normalized by the average luminosity of its surrounding background (I_b) to determine the optical darkness ratio (ODR) which is defined as

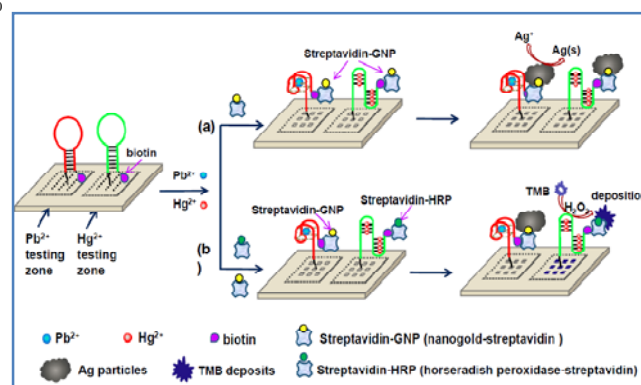
$$ODR = \frac{I_b - I_s}{I_b} \quad (1)$$

Because of the self-correction of the background signal, ODR has been adopted as a convenient measure for quantitative scanometric and colorimetric analysis lately.^{8j, 10} The signal-to-noise ratio (SNR) was calculated by using the following equation:

$$SNR = \frac{\text{mean}}{\text{standard deviation}} = \frac{ODR}{s_b} \quad (2)$$

where ODR and s_b are the mean and standard deviation of the ODR values of the binding strip/spot, respectively. To obtain statistic results, at least three replicates (three strips/spots on the same chip or three replicated chips) were prepared and tested.

Results and Discussion



Scheme 1. Schematic illustration of the DNA hairpin-based colorimetric biochip for the simultaneous detection of Pb²⁺ and Hg²⁺ based on a binding-induced exposure of cryptic site strategy and gold nanoparticle (GNP) enzyme-catalyzed signal enhancement protocols. (a) Single-color staining protocol, (b) dual-color staining protocol.

To identify the ideal probes for these cations, we have designed eight different DNA hairpin strands (Table S1, ESI[†]) and systemically investigated the effect of the stem length, base sequence, and the binding domain on their detection performance. Particularly for the detection of Pb²⁺, we immobilized four DNA hairpin strands (GG-5, GG-6a, GG-6b and GG-7), consisting of the same binding domain but different stem lengths or stem base sequences, on the same plastic substrate as line arrays (three repeats for each probe). Their responses to the blank and sample solutions, containing 50 μ M Pb²⁺ and 50 μ M Hg²⁺, were

examined accordingly. Similarly, we immobilized four thymine (T)-rich DNA hairpin strands (namely, TT-6a, TT-6b, TT-7a and TT-7b) on another plastic substrate as line arrays to determine the optimal probe sequence for the detection of Hg²⁺. Fig. 1(a) and 1(b) show a typical optical image of both chips (after staining), in which the responses of the probes to Pb²⁺ and to Hg²⁺ are represented by the corresponding binding strips. According to the optical darkness ratio (ODR) and signal to-noise ratio (SNR) values corresponding to each design (Fig.S1 and S2, ESI[†]), it is clear that the GG-6b probe shows the best response to Pb²⁺ and the lowest response to Hg²⁺ while the TT-7b probe demonstrates the best response to Hg²⁺ and the lowest response to Pb²⁺. The strong and specific interaction between the two probes (i.e., GG-6b and TT-7b) and the two metal ions (Pb²⁺ and Hg²⁺) were also confirmed by UV-Vis absorption spectroscopy and circular dichroism (CD) spectroscopy; in both cases, the distinct binding-induced probe conformational changes were observed (Fig.S1 and S2, ESI[†]).

The sensitivity and specificity of GG-6b binding to Pb²⁺ and TT-7b binding to Hg²⁺ were then individually evaluated by the chip-based assays using a set of standard solutions. As shown in Fig. 1(c) and 1(d), the two chips for Hg²⁺ and Pb²⁺ detection both display a dynamic response to the different concentrations of their respective ions (from 0.5 nM to 50 μM) by producing distinct binding strips with different darkneses. We have found that the ODR values in the two cases both keep a linear relationship with the logarithmic concentrations of Pb²⁺ and Hg²⁺

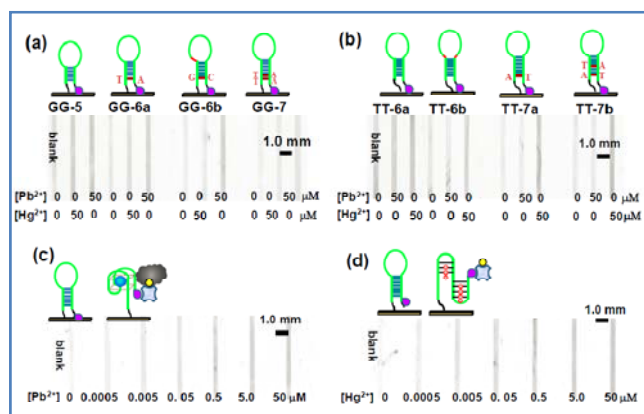


Fig.1 Optimization of DNA hairpin probes for Pb²⁺ and Hg²⁺ detection: representative optical image of the biochip immobilized with (a) four Pb²⁺-sensing probes and (b) four Hg²⁺-sensing probes for detection of Pb²⁺ and Hg²⁺ individually; representative image of the chip showing (c) the responses of GG-6b probes and (d) the responses of TT-7b probes to different concentrations of Pb²⁺ and Hg²⁺, respectively. The insets in (a-d) are the hypothetical conformations of the DNA hairpin probes before and after binding.

over a large range (Fig.S3 and S4, ESI[†]). Given the fact that the

ODR value of the binding strips corresponding to 5.0 nM Pb²⁺ and 5.0 nM Hg²⁺ are both much higher than that of the blanks, the two chips can detect at least as low as 5.0 nM Pb²⁺ and 5.0 Hg²⁺ respectively. Such detectable concentrations are much lower than the maximum allowable level of Pb²⁺ (48 nM) and Hg²⁺ (10 nM) in drinking water recommended by the World Health Organization (WHO),¹¹ indicating that the two chips have the capability to screen Pb²⁺ and Hg²⁺ contamination in common drinking water. In addition, we confirmed that neither the Pb²⁺-sensing chip nor the Hg²⁺-sensing chip were influenced by other common cations in solution, demonstrating their excellent selectivity (Fig.S5 and S6, ESI[†]).

The success of GG-6b and TT-7b probes on a PC chip to detect Pb²⁺ and Hg²⁺ individually allowed us to explore whether the two probes could be employed together, to analyze the two cations simultaneously. To tackle this task, we used a microfluidic channel plate to immobilize GG-6b and TT-7b as probe arrays at different locations of the same chip to form the “Pb²⁺ testing zone” and the “Hg²⁺ testing zone”, respectively. Another microfluidic channel plate was then applied to deliver solutions containing Pb²⁺ and Hg²⁺ across the testing zones in the direction perpendicular to the probe line arrays. With such a design, the recognition events between the two probes and the two target ions occur at the intersections of the microchannels on the second PDMS plate and the preformed probe line arrays, resulting in the formation of 2D binding arrays. Based on color, darkness, and position of the binding spots, this chip can then be used to identify and quantify Pb²⁺ and Hg²⁺ in binary mixtures.

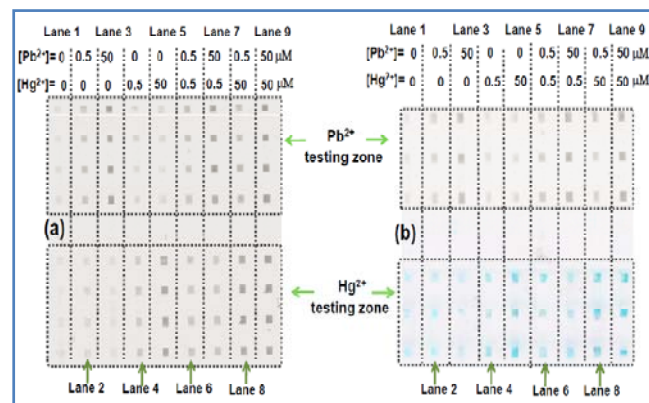


Fig.2 DNA hairpin-based colorimetric biochip for simultaneous detection of Pb²⁺ and Hg²⁺ in lake water: representative optical images of the biochips after (a) single-color staining and (b) dual-color staining, showing the colorimetric responses (represented by the binding spots with different colors or darkneses) of surface-immobilized GG-6b probes (in the Pb²⁺ testing zone) and TT-7b probes (in the Hg²⁺ testing zone) to nine lake water samples containing different concentrations of Pb²⁺ and Hg²⁺.

As a proof-of-concept experiment, we employed this type of biochip to analyze nine lake water samples spiked with different

concentrations of Pb^{2+} (0, 0.5, 50 μM) and Hg^{2+} (0, 0.5, 50 μM). As shown in Fig. 2(a), for the samples containing only Pb^{2+} , distinct binding spots in the Pb^{2+} testing zone were observed, while only very low level signals were detected for these samples in the Hg^{2+} testing zone (lanes 2 and 3), and *vice versa* (low signals for Hg^{2+} -containing solutions in the Pb^{2+} testing zones and high signals in the Hg^{2+} testing zones, lanes 4 and 5). Nevertheless, for the samples containing both Pb^{2+} and Hg^{2+} , distinct binding spots at the corresponding locations in both testing zones (lanes 6-9) were identified. Besides readily distinguishing Pb^{2+} and Hg^{2+} , we were able to visually assess the abundance of Pb^{2+} and Hg^{2+} in the test samples based on the darkness of the binding spots appearing in the two testing zones (Fig. S7, ESI[†]), i.e., the darker the spots, the higher the concentration of the corresponding target ion (lanes 1-9). It should be noted that the interference between Pb^{2+} and Hg^{2+} on this chip is very low and easily recognized. To show the quantitative analysis of the biochip, the ODR values of all the binding spots on the chip are plotted in Fig. S7(b) as a 2D histogram.

Because the binding spots in both testing zones appear grey as a result of silver staining, this may cause confusion in data analysis if the two zones cannot be readily distinguished. To overcome this limitation, we developed a dual-color staining protocol for parallel screening of Pb^{2+} and Hg^{2+} on the same chip. As shown in Fig. 2(b), uniform spots in cyan and grey are present in the Hg^{2+} and Pb^{2+} testing zones, respectively. Here we adapted the horseradish-catalyzed TMB staining and gold nanoparticle-catalyzed silver staining protocol to “develop” the two testing zones separately. Because the color and darkness of the binding spots are easily distinguished, one can readily determine the relative abundances of Pb^{2+} and Hg^{2+} in the test samples (see Fig. S8, ESI[†]).

Considering the potential of this biochip for applications in medical diagnostics, we have also shown that the response of the biochip to both metal cations in human serum and human plasma are as strong as those in the buffer solution. i.e., the darknesses and positions of the binding spots are well correlated with the concentrations of Pb^{2+} and Hg^{2+} in these samples (Fig. S9, ESI[†]).

To further validate its potential application, we have directly compared this method with ICP-MS by testing two industrial water samples (electroplating waste) containing unknown concentrations of Pb^{2+} and Hg^{2+} . In Fig. 3, we have plotted the ODR value as a function of logarithmic concentration; regression equations were obtained for the investigated concentration ranges yielding satisfactory linearity. The fitting ranges are 25 nM to 10 μM for Pb^{2+} ($R^2 = 0.998$) and 50 nM to 10 μM for Hg^{2+} ($R^2 = 0.973$), respectively. As shown in Table S2 (in ESI[†]), the

concentrations of Pb^{2+} and Hg^{2+} determined by the two methods are generally consistent with each other (with maximal relative errors less than 12%), indicating that the colorimetric chips can be used for quantitative detection of these metal cations. Lastly, we have assessed the biochip stability by storing them for different periods of time; the biochip was found to yield a response that accounted for ca. 80% of the original signal after four weeks of storage (Fig.S10, ESI[†]).

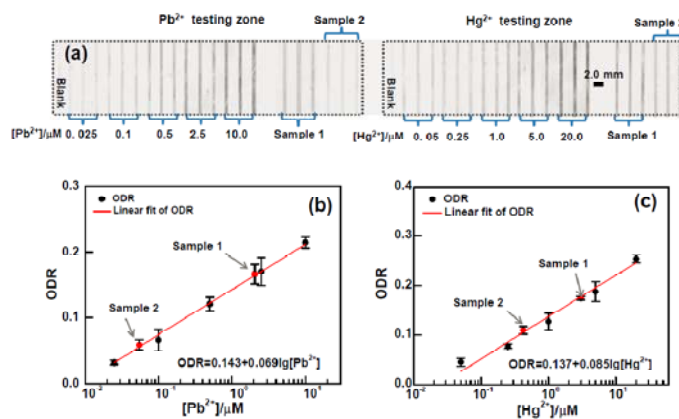


Fig.3 Quantitation of Pb^{2+} and Hg^{2+} in two real-world samples by the chip-based colorimetric method: (a) representative chip image showing the responses of the DNA hairpin-based biochip (GG-6b and TT-7b probes) to a series of standards (containing known concentrations of Pb^{2+} or Hg^{2+}) and to two electroplating waste water samples (containing unknown concentrations of Pb^{2+} and Hg^{2+}); (b-c) dependence of the ODR values on Pb^{2+} and Hg^{2+} concentrations (red dots mark the two waste water samples, and the red line is the best linear fit to the ODR values of the standards). The experimental uncertainties (error bars) shown in (b) and (c) were derived from the replicated strips on the same chip.

Currently, one limitation of this biochip is that the assay conditions (such as, target binding time, blocking protocol and staining time) can significantly influence its analytical result. Therefore, it is imperative to keep all the experimental conditions the same when performing quantitative analysis based on this biochip. Although this biochip has a wide response range (beneficial for on-site pre-screening of real world samples), highly accurate quantitation in the low nM range is still a challenge for it. This is limited by the nature of logarithmic calibration curve (propagation of uncertainty) and the slightly large signal noise associated with the biochip.

90 Conclusion

In summary, a novel binary DNA hairpin-based colorimetric biochip has been developed for on-site and parallel detection of Pb^{2+} and Hg^{2+} in real-world samples. This new biochip incorporates two dually modified DNA hairpin strands containing target-binding domains as probes and employs a binding-induced

1 exposure of cryptic site strategy in conjunction with gold
2 nanoparticle or enzyme-based signal enhancement protocols.
3 Trace amounts of Pb²⁺ and Hg²⁺ (down to 5.0 nM Pb²⁺ and 5.0
4 nM Hg²⁺) were detected in binary mixtures and in real-world
5 samples (lake water, human blood, and industrial waste water),
6 according to the position, darkness and color information
7 associated with the binding spots formed thereon. More
8 importantly, this biochip showed acceptable quantitation
9 accuracy and robust performance over long periods of aging. We
10 believe that it is a promising platform for performing on-site and
11 multiplex analyses of heavy metal ions in real-world samples,
12 augmenting its application potential in medical diagnostics and
13 environmental monitoring.

14 This work was jointly supported by Beijing Science and
15 Technology New Star Project (2010B021), Scientific Research
16 Foundation for Returned Scholars of Ministry of Education of
17 China, the National Natural Science Foundation of China (NSFC,
18 21003012, 21273020, 61174010 and 21233003 (the State Key
19 Program)), and the Natural Science and Engineering Research
20 Council (NSERC) of Canada. Thanking Dr. Eberhard Kiehlmann
21 and Miss Jessica Wong for proofreading the manuscript.

22 Notes and references

23 ^aDepartment of Chemistry, Beijing Normal University, Beijing 100875, P.
24 R. China; E-mail: lyvc@bnu.edu.cn (Y.L.)

25 ^bDepartment of Chemistry, Simon Fraser University, Burnaby, British
26 Columbia V5A1S6, Canada; E-mail: hogan_yu@sfu.ca (H.-Y.)

27 †Electronic Supplementary Information (ESI) available: Experimental
28 details and additional figures. See DOI: 10.1039/b000000x/

- 29 30 1 (a) H.Needleman, *Annu. Rev. Med.*, 2004, **55**, 209–222; (b) Q. R.Wang,
31 D. Kim, D. D.Dionysiou, G. A.Sorial, D. Timberlake, *Environ. Pollut.*,
32 2004, **131**, 323–336.
- 33 2 (a) J. V.Cizdziel, S. Gerstenberger, *Talanta*, 2004, **64**, 918–921; (b) M.
34 Ghaedi, A.Shokrollahi, K.Niknam, E.Niknam, A. Najibi, M.Soylak,
35 *J. Hazard. Mater.*, 2009, **168**, 1022–1027.
- 36 3 (a) A. Ataro, R. I.McCrindle, B. M. Botha, M. E.C.McCrindle, P. P.
37 Ndibewu, *Food Chemistry*, 2008, **111**, 243–248; (b) Y.Li, C.Chen, B.
38 Li, J.Sun, J.Wang, Y.Gao, Y.Zhao, Z.Chai, *J. Anal. At. Spectrom.*,
39 2006, **21**, 94–96.
- 40 4 (a) W.Yantasee, Y. H.Lin, K. Hongsirikarn, G. E. Fryxell, R.
41 Addleman, C.Timchalk, *Environ. Health Persp.*, 2007, **115**, 1683–1690;
42 (b) D. W.Pan, Y.Wang, Z. P.Chen, T. T.Lou, W.Qin, *Anal. Chem.*,
43 2009, **81**, 5088–5094.
- 44 5 (a) Z. Q.Hu, C. S.Lin, X. M. Wang, L.Ding, C. L.Cui, S. F.Liu, H. Y.
45 Lu, *Chem. Commun.*, 2010, **46**, 3765–3767; (c) H. N.Kim, W.X.Ren,
46 J.S.Kim, J.Yoon, *Chem. Soc. Rev.*, 2012, **41**, 3210–3244.
- 47 6 (a) H.Wang, Y. X.Wang, J.Y.Jin, R. H.Yang, *Anal. Chem.*, 2008, **80**,
48 9021–9028; (b) C. W.Liu, C. C.Huang, H. T.Chang, *Anal. Chem.*, 2009,
49 **81**, 2383–2387; (c) R. Freeman, T. Finder, I. Willner, *Angew. Chem.*
50 *Int. Ed.*, 2009, **48**, 7818–7821; (d) J.Du, M.Y.Liu, X. H. Lou, T.Zhao,
51 Z.Wang, Y.Xue, J. L.Zhao, Y. S.Xu, *Anal. Chem.*, 2011, **83**, 225–230;
52 (e) C. L.Hao, L. G.Xua, C. G.Xing, H.Kuang, L. B.Wang, C. L.Xu,
53 *Biosens. Bioelectron.*, 2012, **36**, 174–178; (f) C. H.Chung, J. H.Kim,
54 J.Jung, B. H.Chung, *Biosens. Bioelectron.*, 2013, **41**, 827–832; (g) G.
55 C.Zhu, Y.Li, C. Y.Zhang, *Chem. Commun.*, 2014, **50**, 572–574.
- 56 7 (a) L.Shen, Z.Chen, Y. H.Li, S.He, S. B. Xie, X. D.Xu, Z.W.Liang,
57 X.Meng, Q.Li, Z.W.Zhu, M. X.Li, X. C.Le, Y. H.Shao, *Anal. Chem.*,
58 2008, **80**, 6323–632; (b) Z. Q.Zhu, Y. Y.Su, J.Li, D.Li, J.Zhang, S.
59 P.Song, Y.Zhao, G. X.Li, C. H.Fan, *Anal. Chem.*, 2009, **81**, 7660–7666;
60 (c) S.-J.Liu, H.-G.Nie, J.-H.Jiang, G.-L.Shen, R.-Q. Yu, *Anal.*
Chem., 2009, **81**, 5724–5730; (d) Z. Z.Lin, X. H.Li, H. B. Kraatz, *Anal.*
Chem., 2011, **83**, 6896–6901; (e) M.Zhang, L.Ge, S. G.Ge, M.Yan, J.
H.Yu, J. D.Huang, S. Liu, *Biosens. Bioelectron.*, 2013, **41**, 544–550; (f)
J. Y.Zhuang, L. B.Fu, D. P.Tang, M. D.Xu, G. N. Chen, H. H.Yang,
65 *Biosens. Bioelectron.*, 2013, **39**, 315–319.
- 66 8 (a) J.-S.Lee, C. A.Mirkin, *Anal.Chem.*, 2008, **80**, 6805–6808; (b) J.
67 M.Slocik, J. S.Zabinski, D. M.Phillips, R. R.Naik, *Small*, 2008, **4**,
68 548–551; (c) T.Li, S. J.Dong, E.Wang, *Anal. Chem.*, 2009, **81**, 2144–
69 2149; (d) R.Marc, M. S.Knecht, *Anal. Bioanal. Chem.*, 2009, **394**, 33–
70 46; (e) D.Mazumdar, J. W.Liu, G.Lu, J. Z.Zhou, Y. Lu, *Chem.*
Commun., 2010, **46**, 1416–1418; (f) K. W.Huang, C. J. Yu, W. L.
Tseng, *Biosens. Bioelectron.*, 2010, **25**, 984–989; (g) F.Chai, C.Wang,
T.Wang, L. Li, Z.Su, *ACS Appl. Mater. Interfaces.*, 2010, **2**, 1466–1470;
75 (h) Y. M. Guo, Z.Wang, W. S.Qu, H. W.Shao, X. Y.Jiang, *Biosens.*
Bioelectron., 2011, **26**, 4064–4069; (i) Y. W.Lin, C. C.Huang, H. T.
Chang, *Analyst*, 2011, **136**, 863–871; (j) X. L.Shi, J.Wen, Y. C. Li, Y.
Zheng, J. J.Zhou, X. H.Li, H.-Z.Yu, *ACS Appl. Mater.*
Interfaces., 2014, **6**, 21788–21797.
- 80 9 (a) Y.We, R.Yang, J.-H.Liu, X. J. Huang, *Electrochimica Acta*,
2013, **105**, 218–223; (b) C. W.Lien, Y. T.Tseng, C. C.Huang, H. T.
Chang, *Anal. Chem.*, 2014, **86**, 2065–2072.
- 10 (a) S. Gupta, S. Huda, P.K. Kilpatrick, O. D. Velev, *Anal. Chem.*, 2007,
79, 3810–3820; (b) J. Wen, X.L. Shi, Y.N. He, J.J Zhou, Y.C. Li,
Anal. Bioanal. Chem., 2012, **404**, 1935–1944.
- 85 11. World Health Organization (WHO), Guidelines for drinking-water
quality, 4th Ed.; World Health Organization: Geneva, Switzerland,
2011.